

## Heterostructured Bi<sub>2</sub>Se<sub>3</sub> Nanowires with Periodic Phase Boundaries

Xiaofeng Qiu,<sup>†‡</sup> Clemens Burda,<sup>\*‡</sup> Ruiling Fu,<sup>†</sup> Lin Pu,<sup>§</sup> Hongyuan Chen,<sup>†</sup> and Junjie Zhu<sup>\*†</sup>

Key Laboratory of Analytical Chemistry for Life Science, Department of Chemistry, Nanjing University, Nanjing 210093, PR China, Department of Chemistry, Center for Chemical Dynamics and Nanomaterials Research, Case Western Reserve University, Cleveland, Ohio 44106, and Department of Physics, Nanjing University, Nanjing 210093, PR China

Received July 23, 2004; E-mail: jizhu@nju.edu.cn; burda@case.edu

Recent theoretical studies indicate that phase boundaries in nanowires reduce the lattice thermal conductivity, thus significantly improving the efficiency of thermoelectric materials.<sup>1–3</sup> However, introduction of intrinsic interfaces along the growth axis of nanowires is difficult, from a synthetic perspective which deters the advancement of manufacturing high-performance thermoelectric devices. It is therefore very important to develop new chemical approaches to provide the building blocks for improved thermoelectrics. Here we report a new synthesis of crystalline Bi<sub>2</sub>Se<sub>3</sub> nanowires with periodic phase boundaries between hexagonal and orthorhombic phases.

To date, the best bulk thermoelectric materials at room temperature are alloys of A<sub>2</sub><sup>V</sup>B<sub>3</sub><sup>VI</sup> binary compounds such as Bi<sub>2</sub>Te<sub>3</sub>, Sb<sub>2</sub>Te<sub>3</sub>, Bi<sub>2</sub>Se<sub>3</sub>, which are doped with traces of other elements. This makes Bi<sub>2</sub>Se<sub>3</sub> a good target material for developing heterojunction nanowires that have good potential to improve thermoelectric properties. Previous reports have shown that heterojunction metal nanowires can be achieved by direct electrodeposition in alumina templates.<sup>4,5</sup> However, this method does not generate single-crystalline nanowires, and the junctions are not lattice matched. Lieber and co-workers have developed an alternative metal-catalyzed approach to synthesize heterojunctions between carbon nanotubes and silicon nanowires.<sup>6</sup> On the other hand, Li et al. reported the synthesis of SiC–CNT heterojunctions via a thermal evaporation method.<sup>7</sup> A very successful approach for the synthesis of heterojunction nanowires is to control the flow of semiconductor vapors during the nanostructure growth. Outstanding examples of materials, prepared by using the latter technique, are Si/SiGe superlattice nanowires and InAs/InP heterostructure nanowires.<sup>8,9</sup> However, despite the success of these physical methods in the preparation of heterostructure nanowires the processes are still complicated, highly energy consuming, and very costly. Moreover, the synthesis of V–VI semiconductor heterostructures via these methods is still to be realized.

In recent years, sonochemical and sonoelectrochemical techniques have been extensively used in the synthesis of nanostructure materials.<sup>10–12</sup> During the acoustic cavitation process, very high temperatures (>5000 K), pressures (>20 MPa) and cooling rates (>10<sup>7</sup> K/s) can be achieved upon the collapse of the bubble. Such remarkable environments provide a unique platform for the growth of novel nanostructures.

In this communication we present an alternative sonoelectrochemical route for the formation of striped Bi<sub>2</sub>Se<sub>3</sub> nanowires. The synthesis of Bi<sub>2</sub>Se<sub>3</sub> heterojunction nanowires is adapted from our previous study.<sup>13</sup> First, hexagonal structured Bi<sub>2</sub>Se<sub>3</sub> precursor nanowires were produced via a sonoelectrochemical approach from an aqueous solution of Bi(NO<sub>3</sub>)<sub>3</sub>·5H<sub>2</sub>O and freshly prepared

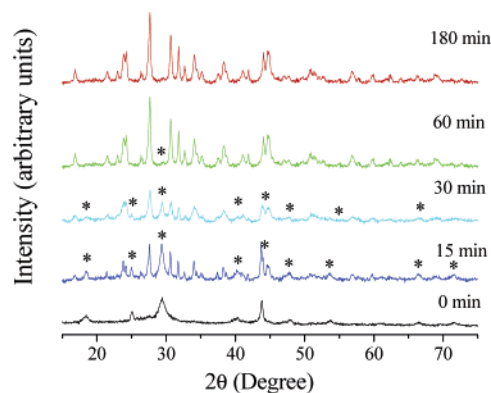


**Figure 1.** XRD patterns of samples after different sonication time. The patterns clearly show the transformation of crystal structures from purely hexagonal before sonication to purely orthorhombic after 3 h of sonication. Peaks marked with \* belong to the hexagonal structure.

Na<sub>2</sub>SeO<sub>3</sub> in the presence of nitrilotriacetic acid (NTA). Then the precursor solution was sonicated without electric current for 1–3 h. For the first step, the sonoelectrochemical setup is similar to that reported before.<sup>14,11</sup> On the other hand, under the current experimental conditions, utilization of a stoichiometric reactant ratio enabled us to produce nanowires of highest purity and crystallinity. We obtained the best crystallized products using current densities in the range of 35.4–53.0 mA/cm<sup>2</sup>. In the second step, the precursor solution was continuously sonicated for 1–3 h. The ultrasound pulse on/off ratio was 9:1 using a 0.6 cm diameter Ti horn at 20 kHz and 60 W/cm<sup>2</sup>. The solutions were centrifuged, and the precipitates were washed three times with water and ethanol and then dried.

Figure 1 shows the XRD patterns (Philips X'pert) of the Bi<sub>2</sub>Se<sub>3</sub> powder extracted after different sonication times. The XRD measurements show that the crystal structure changed drastically during the first hour of sonication. Before sonication, the XRD pattern exhibited a pure hexagonal crystal structure (JCPDS file: 33-214), and subsequent peaks of newly formed orthorhombic crystals (JCPDS file: 77-2016) started to emerge after 15 min of sonication.

The intensities of the original peaks were reduced after 30 min, which indicated a phase change in the sonication product. After 1 h of sonication, the peaks of the hexagonal crystals almost disappeared, and after 3 h, the pattern showed a purely orthorhombic crystal structure.

Using transmission electron microscopy (TEM, JEOL-JEM 200CX, 200kV) we could show that the morphology of Bi<sub>2</sub>Se<sub>3</sub> changed from sheetlike structures into nanowires as sonication occurred. After 3 h of sonication, most of the material turned into nanowires. The diameter of the nanowires varies from 10 to 40 nm, and the lengths of the nanowires range from 500 nm to several micrometers. Besides the formation of nanowires, we

<sup>†</sup> Department of Chemistry, Nanjing University.

<sup>‡</sup> Case Western Reserve University.

<sup>§</sup> Department of Physics, Nanjing University.

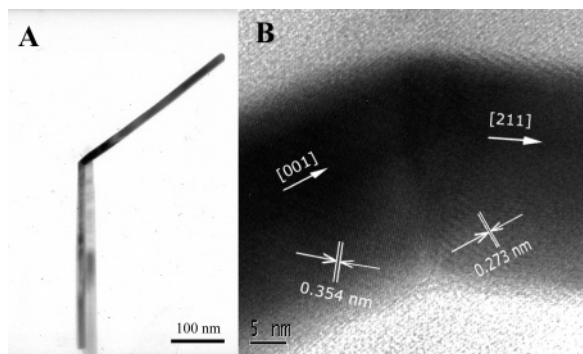


**Figure 2.** (A) TEM image of a heterostructured  $\text{Bi}_2\text{Se}_3$  nanowire. (B) HRTEM image of the heterojunction, the lattice spacing of phase 1 is 0.273 nm which corresponds to the [211] plane of the orthorhombic phase; the lattice spacing of phase 2 is 0.354 nm, which corresponds to the [001] plane of the hexagonal phase.

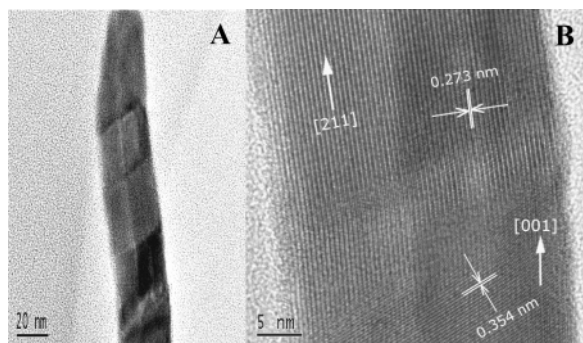


**Figure 3.** (A) TEM of bismuth selenide multiple-heterojunction nanowire with periodic phase boundaries; the thickness of the nanowire is 29.2 nm, and the aspect ratio is 13.2. (B) HRTEM of the nanowire junction; lattice constant of phase 1 corresponds to orthorhombic  $\text{Bi}_2\text{Se}_3$  along the [211] direction; the lattice constant of phase 2 corresponds to hexagonal  $\text{Bi}_2\text{Se}_3$  along the [001] direction.

noticed a very interesting phenomenon that some of the nanowires form a junction structure. As shown in Figure 2A, a nanowire junction with sharp interface can be clearly observed from the TEM image. Such structures start to emerge after 15 min and exist in all the samples afterward. Since the formation of the junction occurred simultaneously with the phase transformation, it seemed plausible that such structures could be a heterogeneous nanowire composed of two distinct phases of  $\text{Bi}_2\text{Se}_3$ . High-resolution TEM (HRTEM, using a JEOL JEM 2010, 400kV) verified our assumption. Figure 2B shows the lattice structure of the junction. The lattice spacing indicates that the junction was formed by two different phases of  $\text{Bi}_2\text{Se}_3$ . As predicted by Dresselhaus and co-workers<sup>1</sup> wire boundary and interfaces along the nanowire will block the phonon transport, hence significantly reducing the lattice thermal conductivity, which is important to enhance the thermoelectric figure of merit.<sup>2</sup>

Furthermore, in the longer-sonicated samples, we found an even more exciting product—multijunction nanowires (Figure 3A). The pulsed ultrasound produced distinct phases within the nanowires. The length of each phase is about 30 nm. HRTEM (Figure 3B) characterization proved that the neighboring phase blocks are

formed of hexagonal and orthorhombic  $\text{Bi}_2\text{Se}_3$  along the [001] and [211] planes, respectively. The multijunction nanowire exhibits a characteristic ABAB superstructure. Thus, heterosuperstructures were synthesized along the growth axis of the nanowires. The sharp interfaces could benefit from the pulsed mode. The periodic structure may arise from stacking faults.<sup>15</sup> Temperature could be a possible reason responsible for the formation of heterojunctions.<sup>16</sup> Elaborated ultrasound conditions can be a strategy for higher yield. Although the yield of multijunction nanowires is difficult to determine ( $\sim 10\%$ ), the number of the multijunction nanowires was proportional to the sonication time as well as the sonication intensity. This trend has been verified for several times and is well reproducible. The pulsed mode was found to improve the control over the thickness of the layers. However, too long sonication times and too high intensities pose a risk of breaking the wires. Similar structures were found for other  $\text{A}_2\text{VB}_3$  binary compounds using the same approach.

In conclusion, we have successfully synthesized single- and multiple-heterojunction nanowires with diameters of 10–40 nm, by a simple electrically assisted sonochemical method in aqueous solution at room temperature. Such a chemical approach provides a promising way to synthesize high-performance building blocks for improved devices. By properly controlling the reaction conditions and reactants, this method opens a new strategy toward the fabrication of one-dimensional superlattices in nanowires under ambient conditions.

**Acknowledgment.** J.J.Z., L.P., and H.Y.C. acknowledge support from NSFC (Grants 20325516, 60206001, 90206037), JS-STF (BK2002411), and 863 Project (2003AA302740). C.B. acknowledges support from NSF (CHE-0239688) and PRI (Ohio Board of Regents).

## References

- (1) Lin, Y. M.; Dresselhaus, M. S. *Phys. Rev. B* **2003**, *68*, 075304–075314.
- (2) Li, D. Y.; Wu, Y. Y.; Fan, R.; Yang, P. D.; Majumdar, A. *Appl. Phys. Lett.* **2003**, *83*, 3186–3188.
- (3) Dresselhaus, M. S.; Lin, Y. M.; Cronin, S. B.; Rabin, O.; Black, M. R.; Dresselhaus, D.; Koga, T. *Semicond. Semimet.* **2001**, *71*, 1–121.
- (4) Nicewarner-Pena, S. R.; Freeman, R. G.; Reiss, B. D.; He, L.; Pena, D. J.; Walton, L. D.; Cromer, R.; Keating, C. D.; Natan, M. J. *Science* **2001**, *294*, 137–141.
- (5) Martin, B. R.; Dermody, D. J.; Reiss, B. D.; Fang, M.; Lyon, L. A.; Natan, M. J.; Mallouk, T. E. *Adv. Mater.* **1999**, *11*, 1021–1025.
- (6) Hu, J.; Ouyang, M.; Yang, P.; Lieber, C. M. *Nature* **1999**, *399*, 48–51.
- (7) Li, Y.; Bando, Y.; Golberg, D. *Adv. Mater.* **2004**, *16*, 93–96.
- (8) Wu, Y. Y.; Fan, R.; Yang, P. D. *Nano Lett.* **2002**, *2*, 83–86.
- (9) Bjork, M. T.; Ohlsson, J. B.; Sass, T.; Persson, A. I.; Thelander, C.; Magnusson, M. H.; Deppert, K.; Wallenberg, L. R.; Samuelson, L. *Nano Lett.* **2002**, *2*, 87–89.
- (10) Gedanken, A.; *Ultrason. Sonochem.* **2004**, *11*, 47–55.
- (11) Mastai, Y.; Polsky, R.; Koltypin, Y.; Gedanken, A.; Hodes, G. *J. Am. Chem. Soc.* **1999**, *121*, 10047–10052.
- (12) Mdleleni, M. M.; Hyeon, T.; Suslick, K. S. *J. Am. Chem. Soc.* **1998**, *120*, 6189–6190.
- (13) Qiu, X. F.; Zhu, J. J.; Pu, L.; Shi, Y.; Zheng, Y. D.; Chen, H. Y. *Inorg. Chem. Commun.* **2004**, *7*, 319–321.
- (14) Qiu, X. F.; Xu, J. Z.; Zhu, J. M.; Zhu, J. J.; Xu, S.; Chen, H. Y. *J. Mater. Res.* **2003**, *18*, 1399–1404.
- (15) Manna, L.; Scher, E. C.; Alivisatos, A. P. *J. Am. Chem. Soc.* **2000**, *122*, 12700–12706.
- (16) Manna, L.; Milliron, D. J.; Meisel, A.; Scher, E. C.; Alivisatos, P. A. *Nat. Mater.* **2003**, *2*, 382–385.

JA045556R